1521-0111/94/5/1298–1309$35.00
MOLECULAR PHARMACOLOGY

https://doi.org/10.1124/mol.118.112490
Mol Pharmacol 94:1298–1309, November 2018

Utility of an "Allosteric Site-Impaired" M_2 Muscarinic Acetylcholine Receptor as a Novel Construct for Validating Mechanisms of Action of Synthetic and Putative Endogenous Allosteric Modulators [S]

Ee Von Moo, Patrick M. Sexton, Arthur Christopoulos, and Celine Valant

Drug Discovery Biology, Monash Institute of Pharmaceutical Sciences, Monash University, Parkville, Victoria, Australia

Received March 21, 2018; accepted September 10, 2018

ABSTRACT

Muscarinic acetylcholine receptors (mAChRs) are exemplar models for understanding G protein–coupled receptor (GPCR) allostery, possessing a "common" allosteric site in an extracellular vestibule (ECV) for synthetic modulators including gallamine, strychnine, and brucine. In addition, there is intriguing evidence of endogenous peptides/proteins that may target this region at the M_2 mAChR. A common feature of synthetic and endogenous M_2 mAChR negative allosteric modulators (NAMs) is their cationic nature. Using a structure-based approach, we previously designed a mutant M_2 mAChR (N410K+T423K) to specifically abrogate binding of ECV cationic modulators (Dror et al., 2013). Herein, we used this "allosteric site-impaired" receptor to investigate allosteric interactions of synthetic modulators as well as basic peptides (poly-L-arginine, endogenously produced protamine, and major basic protein). Using [^{3}H]*N*-methylscopolamine equilibrium and kinetic binding and functional assays of guanosine 5′-*O*-[γ-thio]triphosphate [^{35}S] binding and extracellular signal-regulated kinases 1 and 2 phosphorylation, we found modest effects of the mutations on potencies of orthosteric antagonists and an increase in the affinity of the cognate agonist, acetylcholine, likely reflecting the effect of the mutations on the access/egress of these ligands into the orthosteric pocket. More importantly, we noted a significant abrogation in affinity for all synthetic or peptidic modulators at the mutant mAChR, validating their allosteric nature. Collectively, these findings provide evidence for a hitherto-unappreciated role of endogenous cationic peptides interacting allosterically at the M_2 mAChR and identify the allosteric site-impaired GPCR as a tool for validating NAM activity as well as a potential candidate for future chemogenetic strategies to understand the physiology of endogenous allosteric substances.

Introduction

G protein–coupled receptors (GPCRs) participate in all aspects of physiology and are the largest class of drug targets (Santos et al., 2017). However, in many instances, it can be extremely difficult to specifically target one GPCR subtype over another. One such example is the muscarinic acetylcholine receptor (mAChR) family (Caulfield and Birdsall, 1998). Dysfunction of mAChRs is involved in numerous disorders (Abrams et al., 2006; Langmead et al., 2008), and consequently, several Food and Drug Administration–approved mAChR-targeting drugs have been developed. Unfortunately, all of these medicines interact with the orthosteric site, which is completely conserved between the five mAChRs (Thal et al., 2016) and can thus underlie unacceptable adverse effects (Wess et al., 2007). As a consequence, discovery efforts have shifted toward targeting fewer conserved allosteric sites on the mAChRs to overcome such selectivity challenges (Christopoulos, 2002).

Historically, the M_2 mAChR has been one of the best-studied GPCRs in terms of allosteric targeting and remains an exemplar model for understanding mechanisms of allostery, particularly with regards to small-molecule negative allosteric modulators (NAMs) and, more recently, positive allosteric modulators (Christopoulos et al., 1998; Gregory et al., 2010; Valant et al., 2012; Dror et al., 2013; Kruse et al., 2013, 2014). One common feature of numerous classes of M_2 mAChR–preferring NAMs is that they are cationic molecules (Gregory et al., 2007), and recent structural biology breakthroughs have provided mechanistic insights into why this is the case. Specifically, the mAChRs possess an extracellular vestibule (ECV) that constitutes the

This work was funded by the National Health and Medical Research Council of Australia (NHMRC) [Program Grant APP1050083; Project Grant APP1082318] and by the Australian Research Council [Grant FT140100114]. A.C. is a Senior Principal Research Fellow of the NHMRC, P.M.S. is a Principal Research Fellow of the NHMRC, C.V. is an Australian Research Council Future Fellow, and E.V.M. is a recipient of an Australian Postgraduate Award.
https://doi.org/10.1124/mol.118.112490.
[S] This article has supplemental material available at molpharm.aspetjournals.org.

ABBREVIATIONS: ACh, acetylcholine; CHO, Chinese hamster ovary; DMEM, Dulbecco's modified Eagle's medium; ECV, extracellular vestibule; ERK1/2, extracellular signal-regulated kinases 1 and 2; FBS, fetal bovine serum; GPCR, G protein–coupled receptor; Gpp(NH)p, Guanosine 5′-[β,γ-imido]triphosphate; [^{3}H]NMS, *N*-[^{3}H]methylscopolamine; LDH, lactate dehydrogenase; mAChR, muscarinic acetylcholine receptor; MBP, major basic protein; NAM, negative allosteric modulator; PLA, poly-L-arginine; [^{35}S]GTPγS, guanosine 5′-*O*-[γ-thio]triphosphate [^{35}S]; TM, transmembrane; WT, wild type.

location of a topographically "common" allosteric site defined by a combination of both conserved and nonconserved amino acids as well as differences in charge distribution; the M_2 mAChR shows the highest degree of electronegativity, of all mAChRs, in this region (Haga et al., 2012; Kruse et al., 2012; Thal et al., 2016).

Interestingly, GPCR allosteric sites have traditionally been regarded as domains assisting receptor folding, trafficking, and structural integrity, with the serendipitous advantage of possessing residues that can also be targeted by exogenous synthetic molecules (van der Westhuizen et al., 2015). Although this is most likely to be the case in the majority of instances, the widespread presence of GPCR allosteric sites suggests that there may also be a role for some of these sites in the actions of hitherto-unappreciated endogenous allosteric ligands (van der Westhuizen et al., 2015; Changeux and Christopoulos, 2016 [retracted]). That is, some allosteric sites may act as "orphan" binding sites for endogenous ligands. It is thus noteworthy that the polycationic human eosinophil major basic protein (MBP), a peptide that constitutes ~50% of the inflammatory peptides released following infiltration and degranulation of eosinophils (Ackerman et al., 1983), can bind to the M_2 mAChR in a potentially allosteric fashion (Jacoby et al., 1993). In addition to MBP, other basic peptides, such as protamine, dynorphin A (1-13), and myelin basic protein (Hu et al., 1992; Hu and el-Fakahany, 1993), have been suggested to negatively modulate the binding of the orthosteric antagonist radioligand *N*-[^{3}H]methylscopolamine ([^{3}H]NMS) at the M_2 mAChR. However, the degree of inhibition exhibited by the latter peptides is substantial and thus indicative of either high negative cooperativity or a competitive mode of interaction.

Recently, using a combination of molecular dynamic simulations and structure-function analyses, we identified two key residues in the ECV of the M_2 mAChR, Asn410$^{6.58}$ and Thr423$^{7.36}$ (superscripts refer to Ballesteros-Weinstein residue numbering), as playing a vital role in the binding of synthetic cationic NAMs, with mutation of both of these residues to lysine (N410K+T423K) significantly decreasing the binding affinity of the prototypical NAMs, gallamine and heptane-1,7-bis(dimethyl-3′phthalimodipropylammonium), via charge-charge repulsion (Dror et al., 2013). Based on this finding, it is possible that this mutant receptor may prove useful for studying and validating the mode of action of other classes of cationic modulators, either exogenous or endogenous, at the M_2 mAChR. Thus, the aim of the current study was to perform a rigorous pharmacological characterization of the binding and functional properties of this "allosteric site-impaired" mutant receptor using a range of orthosteric and allosteric ligands, including small molecules and basic cationic peptides. We found that the mutant, although having modest effects on the actions of orthosteric ligands, has a greater impact on the binding and function of allosteric modulators, highlighting its potential as a useful construct not only for validating the allosteric ligand mode of action but also as a potential candidate for future utility in chemogenetic strategies for unmasking a role of putative endogenous allosteric substances of the M_2 mAChR.

Materials and Methods

Materials. Dulbecco's modified Eagle's medium (DMEM) and fetal bovine serum (FBS) were from Invitrogen (Carlsbad, CA) and JRH Biosciences (Lenexa, KS), respectively. Hygromycin was purchased from Roche Applied Science (Manheim, Germany). The AlphaScreen SureFire phosphorylated extracellular signal-regulated kinases 1 and 2 (ERK1/2) assay kits were obtained from TGR Biosciences (Adelaide, SA, Australia). The AlphaScreen streptavidin donor beads and anti-IgG (protein A) acceptor beads used for phosphorylated ERK1/2 detection, AlphaScreen reagents, 384-well ProxiPlates, [^{3}H]NMS (specific activity, 70.0 Ci/mmol), and guanosine 5′-*O*-[γ-thio]triphosphate [^{35}S] ([^{35}S]GTPγS; specific activity, 1250 Ci/mmol) were purchased from PerkinElmer Life Sciences (Waltham, MA). Myelin basic protein and poly-L-arginine were purchased from Sigma-Aldrich (St. Louis, MO), protamine was purchased from Sapphire Bioscience (Redfern, NSW, Australia), and major basic protein was purchased from Cusabio (College Park, MD). All other chemicals were from Sigma-Aldrich and were of analytical grade.

Cell Culture. FlpIn–Chinese hamster ovary (FlpIn-CHO) cells, stably transfected with the human wild-type (WT) or N410K+T423K M_2 mAChRs, were generated as previously described (Dror et al., 2013). The cells were grown and maintained in DMEM supplemented with 5% (v/v) FBS and 100 μg/ml hygromycin-B. Cells were kept in a humidified incubator at 37°C containing 5% CO_2, 95% O_2.

Whole-Cell [^{3}H]NMS Equilibrium Binding Assay. FlpIn-CHO cells stably expressing human muscarinic M_2 receptors (WT or N410K+T423K) were seeded into white opaque IsoPlates (Perkin Elmer Life Sciences, Waltham, MA) at 2.5×10^5 cells per well and then grown at 37°C for 20−24 hours. Cells were washed once with phosphate-buffered solution, 100 μl per well, followed by the addition of 80 μl per well of binding buffer (20 μM HEPES, 10 μM $MgCl_2$, and 100 μM NaCl, pH 7.4) supplemented with 0.1% bovine serum albumin. All ligands were diluted in binding buffer at 10× their required final concentrations, and 10 μl per well was added. Nonspecific binding was determined using 100 μM atropine. For both the wild-type and the N410K+T423K M_2 receptors, cells were equilibrated at 21°C for 4 hours with orthosteric ligand [acetylcholine (ACh) and atropine] or allosteric ligand (gallamine, strychnine, brucine, protamine, poly-L-arginine, or MBP) in the presence of a K_D concentration of [^{3}H]NMS (~0.1 nM) in a total volume of 100 μl per well. Assays were terminated by removal of the drug-containing buffer, followed by 2× 50-μl washes per well with ice-cold 0.9% NaCl solution and addition of 100 μl per well of Optiphase Supermix scintillation liquid (Perkin Elmer Life Sciences). The levels of remaining bound radioligand and, therefore, the degree of specific radioligand inhibition were measured in disintegrations per minute on the Microbeta2 LumiJET 2460 microplate counter (PerkinElmer).

Whole-Cell [^{3}H]NMS Dissociation Kinetic Binding Assay. Cells expressing either the human WT or N410K+T423K M_2 receptors were plated and washed as described earlier. Cells were then equilibrated with [^{3}H]NMS (~0.1 nM) for 2 hours at 21°C. Atropine (100 μM) alone or in the presence of a single (high) concentration of allosteric ligands (see *Results*) was then added at various time points to prevent the reassociation of [^{3}H]NMS with the receptor. Termination of the assay and determination of radioactivity were performed as described earlier.

Whole-Cell [^{3}H]NMS Association Kinetic Binding Assay. To determine the association rate constant (k_{on}) of the radioligand, four different concentrations of [^{3}H]NMS (~0.1, 0.3, 0.6, and 1 nM) were used. Cells expressing either the human WT or N410K+T423K M_2 receptors were plated and washed as described earlier. Association was initiated by the addition of [^{3}H]NMS at various time points. Termination of the assay and determination of radioactivity were performed as described earlier.

Membrane-Based [^{3}H]NMS Equilibrium Binding Assay. Cell membranes were prepared and stored as described previously (Valant et al., 2012). Membrane homogenates (20 μg) were incubated in a 1-ml total volume of binding buffer containing [^{3}H]NMS (0.5 nM) and a range of concentrations of ACh at 37°C for 60 minutes. These experiments were performed in both the absence and presence of guanine nucleotides with 100 μM Gpp(NH)p (Guanosine 5′-[β,γ-imido]triphosphate). Nonspecific binding was defined using 10 μM atropine. The assay was terminated by rapid filtration through Whatman GF/B filters using a cell harvester (Brandel Inc., Gaithersburg, MD). Filters were washed three times with 3-ml aliquots of ice-cold 0.9% NaCl solution and dried before being transferred to polypropylene

vials with 4 ml of scintillation mixture (Ultima Gold; PerkinElmer). Vials were then left to stand until the filters became uniformly translucent before radioactivity was determined using scintillation counting on a liquid scintillation analyzer (Tri-Carb 290 TR; PerkinElmer).

[^{35}S]GTPγS Binding Assay. Membrane homogenates (20 μg) were equilibrated in a 500-μl total volume of binding buffer containing 10 μM GDP, in the presence of either increasing concentrations of ACh or an EC_{70} concentration of ACh and increasing concentrations of allosteric ligands, at 30°C for 90 minutes. After this time, 50 μl of [^{35}S]GTPγS (300 pM) was added, and incubation continued for another 30 minutes at 30°C. The assay was terminated as described earlier.

ERK1/2 Phosphorylation Assay. FlpIn-CHO cells, either nontransfected or stably expressing human WT or N410K+T423K M_2 receptors, were seeded into transparent 96-well plates at 2×10^5 cells per well and grown for 6 hours. Cells were then washed once with phosphate-buffered solution and incubated with 80 μl of serum-free DMEM at 37°C overnight (16−18 hours) to allow FBS-stimulated phosphorylated ERK1/2 levels to subside. All ligands were diluted in FBS-free media at 10× their required final concentrations, and 10 μl of drugs was added to induce stimulation. Initial ERK1/2 phosphorylation time-course experiments were performed to determine the time at which ERK1/2 phosphorylation was maximal after stimulation by ligands. For ACh-stimulated concentration-response experiments, cells were incubated at 37°C with ACh for the 5 minutes required to achieve peak response. For interaction experiments, cells were incubated at 37°C with 10 μl per well of antagonists or allosteric modulators for 20 minutes prior to agonist stimulation with an EC_{70} concentration of ACh for 5 minutes. In all experiments, 10% FBS was used as a positive control. Agonist-stimulated ERK1/2 phosphorylation was terminated by the removal of drugs and the addition of 100 μl per well of SureFire lysis buffer. The cell lysates were agitated for 5 minutes. Following agitation, 10 μl of cell lysates was transferred into a 384-well white opaque OptiPlate (Perkin Elmer Life Sciences), followed by addition of 8.5 μl of a solution of reaction buffer/activation buffer/acceptor beads/donor beads at a ratio of 6/1/0.03/0.03 (v/v/v/v) under low-light conditions. The plates were then incubated at 37°C in the dark for 1 hour, and fluorescence was measured on a FusionAlphaScreen plate reader (PerkinElmer) using standard AlphaScreen settings.

Lactate Dehydrogenase Cytotoxic Assay. FlpIn-CHO cells stably expressing human WT M_2 receptors were seeded at 10,000–15,000 cells/well in transparent 96-well plates and grown overnight at 37°C, 5% CO_2. The next day, the cells were incubated with 10 μl of drug treatment, including spontaneous (10 μl of ultra-pure sterile water) and maximum (10 μl of lysis buffer) lactate dehydrogenase (LDH) controls, for 60 minutes at 37°C. Fifty microliters of medium from each well, including medium controls of serum-free DMEM and 5% FBS DMEM, was then transferred to a fresh transparent 96 well tissue culture plate. Fifty microliters of reaction mixture was then added into each well. Upon gentle agitation, the plate was incubated at room temperature for 30 minutes in low-light conditions. Fifty microliters of stop solution was then added into the plate and mixed by gently tapping to prevent bubbles from forming. Absorbance was measured using FLEXstation 3B (490 and 680 nm; Molecular Devices, San Jose, CA). LDH activity was determined by subtracting the 680-nm absorbance value from the 490-nm absorbance value (LDH at 490 nm − LDH at 680 nm). Percentage of cytotoxicity (%cytotoxicity) was calculated using the following equation:

$$\%\text{cytotoxicity} = \left[\frac{(\text{treated LDH} - \text{spontaneous LDH})}{(\text{max LDH} - \text{spontaneous LDH})}\right] * 100 \quad (1).$$

Data Analysis. Computerized nonlinear regression was performed using Prism 7 (GraphPad Software, San Diego, CA). Total and nonspecific [^{3}H]NMS binding data were globally fitted to a one-site saturation binding model to derive estimates of the radioligand equilibrium dissociation constant (K_D) and the maximal density of binding sites (B_{max}) for the human WT and the N410K+T423K M_2 mAChRs. Dissociation kinetic data were fitted to a one-phase exponential decay function to derive the apparent rate constant of dissociation (k_{off}) in the absence or presence of each compound. [^{3}H]NMS association data were globally fitted to the following equation to determine a single best-fit estimate for k_{on}:

$$K_{ob} = [L] \cdot k_{on} + k_{off} \quad (2)$$

where L is the concentration of [^{3}H]NMS in nanomolars, and K_{ob} is the observed rate constant.

Radioligand inhibition binding data with atropine and ACh were empirically fitted to either a one-site or two-site/state inhibition mass action curve to determine inhibitor potency (IC_{50}) estimates, which were then converted to K_I values (Cheng and Prusoff, 1973) as appropriate. Radioligand equilibrium binding curves for interaction with allosteric ligands were fitted to an allosteric ternary complex model (eq. 3) to derive estimates of allosteric modulator affinity (K_B) and cooperativity between the compound and radioligand (α), where $\alpha > 1$ denotes positive cooperativity, $0 < \alpha < 1$ denotes negative cooperativity, and $\alpha = 1$ denotes neutral cooperativity (Christopoulos and Kenakin, 2002):

$$E = \frac{B_{max}[A]}{[A] + (K_A)\left(\frac{K_B + [B]}{K_B + \alpha[B]}\right)} \quad (3)$$

where K_A and K_B represent the equilibrium dissociation constant of the radioligand and competing ligand, respectively, and [A] and [B] denote their concentrations. B_{max} is the relative receptor expression.

Concentration-response curves to the agonist, ACh, were fitted to the following three-parameter dose-response curve equation:

$$Y = \text{basal} + \frac{E_m - \text{basal}}{1 + 10^{(\log EC_{50} - [A])}} \quad (4)$$

where E_m is the maximal possible response of the system, basal is the basal level of response in the absence of agonist, [A] is the concentration of the orthosteric agonist, and EC_{50} is the concentration of the agonist required to generate 50% of response in the absence of allosteric ligand. Functional interaction between orthosteric agonist and orthosteric antagonist was fitted to a logistic equation of competitive agonist-antagonist interaction (Draper-Joyce et al., 2018):

$$E = \text{basal} + \frac{E_m - \text{basal}}{1 + \left(\frac{10^{\log EC_{50}\left[1 + \left(\frac{[B]}{10^{-pA_2}}\right)\right]^s}}{[A]}\right)^{n_H}} \quad (5)$$

where E_m is the maximal possible response of the system; basal is the basal level of response in the absence of agonist; [A] and [B] are the concentrations of the orthosteric agonist and allosteric modulator, respectively; EC_{50} is the concentration of the agonist required to generate 50% of response in the absence of allosteric ligand; s represents the Schild slope for the antagonist; pA_2 represents the negative logarithm of the molar concentration of antagonist that makes it necessary to double the concentration of agonist needed to elicit the original submaximal response obtained in the absence of antagonist; and n_H denotes the Hill slope factor, which was held constant at 1. For this analysis, [A] was fixed as a constant at the molar agonist concentration (EC_{70}) present in the assay.

Functional studies for the interaction of orthosteric agonist and allosteric modulator were fitted to an allosteric ternary complex model (May et al., 2007):

$$E = \frac{E_m \cdot [A]}{[A] + [EC_{50}]\left(\frac{1 + \frac{[B]}{K_B}}{1 + \frac{\alpha\beta[B]}{K_B}}\right)} \quad (6)$$

where E_m is the maximum possible response for the system; [A] and [B] are the concentrations of the orthosteric agonist and allosteric modulator, respectively; EC_{50} is the concentration of the agonist

required to generate 50% of response in the absence of allosteric ligand; α is the cooperativity factor (as described earlier); and K_B is the equilibrium dissociation constant of the allosteric modulator. For this analysis, [A] was fixed as a constant at the molar agonist concentration (EC_{70}) present in the assay. This equation assumes that ACh remains a full agonist in the presence of all concentrations of allosteric modulator.

All affinities, potencies, efficacies, and cooperativity parameters were estimated as logarithms (Christopoulos, 1998). Results are expressed as means ± S.E.M. unless otherwise stated. Statistical analyses were by Student's *t* test or one-way analysis of variance using Dunnett's multiple post-test, as appropriate. A value of $P < 0.05$ was considered statistically significant.

Results

Characterization of the Binding and Kinetic Properties of Orthosteric Antagonist, [^{3}H]NMS, at the WT and N410K+T423K M_2 mAChR. Initial equilibrium saturation binding experiments using the hydrophilic orthosteric antagonist, [^{3}H]NMS, were performed to determine radioligand affinity (pK_D) and cell-surface expression (B_{max}) of the human WT or N410K+T423K mutant M_2 mAChRs, each stably expressed in FlpIn-CHO cells. In agreement with our initial study (Dror et al., 2013), the estimated radioligand pK_D values obtained for the N410K+T423K M_2 mAChR were not significantly different ($P > 0.05$) from the WT values (Fig. 1A; Table 1). In contrast, the B_{max} value of the N410K+T423K mutant M_2 mAChR (86,180 ± 12,230 sites per cell; $n = 6$) was significantly ($P < 0.05$) lower than for the WT receptor (191,631 ± 25,000 sites per cell; $n = 6$) by ~50% (Fig. 1B).

Subsequent experiments determined the kinetic rate constants for radioligand binding at the M_2 mAChR constructs, initially focusing on the radioligand dissociation rate constant, k_{off}. In comparison with the WT receptor, the dissociation rate of [^{3}H]NMS was significantly slower ($P < 0.05$) at the N410K+T423K M_2 mAChR by approximately 6-fold (Fig. 1C; Table 1), suggesting that the mutation of the two residues in the ECV, which are located along the path used by [^{3}H]NMS to reach and exit the orthosteric binding pocket, affected the process of dissociation of the antagonist. Since the equilibrium dissociation constant (K_D) of a ligand is the ratio of its dissociation to association rate constants ($K_D = k_{off}/k_{on}$), we anticipated that the association rate of [^{3}H]NMS would thus also be significantly different between the two receptor constructs. To experimentally determine this value, we performed radioligand association experiments in the presence of increasing concentrations of [^{3}H]NMS, ranging from 0.1 to 1 nM (Fig. 1, D and E), and globally fitted the entire family of curves to eq. 2, with the value of k_{off} fixed to that determined in the dissociation kinetic experiments. As shown in Table 1, the results of this analysis confirmed that the estimated [^{3}H]NMS k_{on} for the WT receptor was significantly higher than at the double-mutant receptor by approximately 3-fold, thus accounting for the minimal effect (~2-fold) on affinity of the radioligand at both constructs at equilibrium. Indeed, the calculated affinity value of the radioligand using the rate constants was only ~3-fold different from the value estimated directly from equilibrium saturation binding experiments (Table 1).

Characterization of Binding and Signaling Properties of Prototypical Orthosteric Ligands at the N410K+T423K M_2 mAChR. To further characterize the pharmacological properties of the N410K+T423K M_2 mAChR, we next investigated the binding and functional properties of two

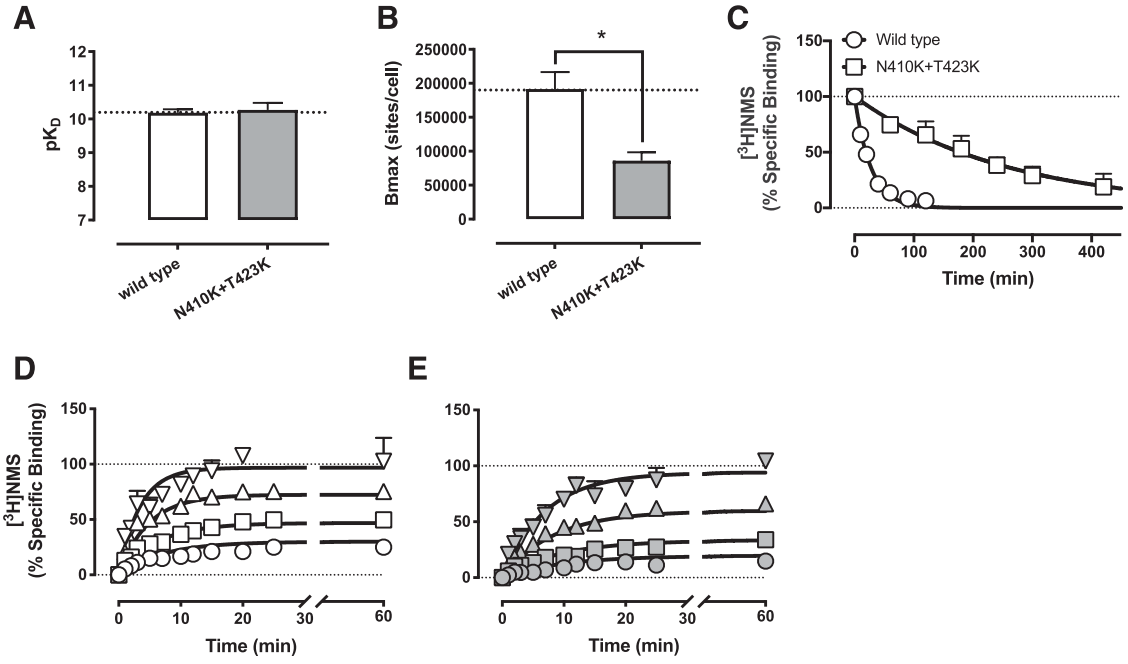

Fig. 1. Binding properties of [^{3}H]NMS at the wild-type and N410K+T423K M_2 mAChR. (A) Affinity estimates for [^{3}H]NMS (as negative logarithms of the dissociation constant, K_D). (B) Receptor expression (B_{max}; sites per cell) of N410K+T423K M_2 mAChR compared with the wild-type receptor. (C) [^{3}H]NMS dissociation from the N410K+T423K M_2 mAChR compared with the wild-type receptor. Association of increasing concentrations of [^{3}H]NMS (○, 0.1 nM, □, 0.3 nM, △, 0.6 nM, ▽, 1 nM) at the wild type (D) or N410K+T423K (E) M_2 mAChR. Data points represent the mean ± S.E. obtained from three to five experiments conducted in duplicate. *Statistically significant when compared with the corresponding value in the wild-type M_2 mAChR, Student's *t* test ($P < 0.05$).

TABLE 1

Equilibrium and kinetic parameter estimates for [^{3}H]NMS at the WT and N410K+T423K M_2 mAChRs

Values represent the mean ± S.E. from at least three experiments performed in duplicate.

	WT	N410K+T423K	n^a
Equilibrium pK_D[b]	10.18 ± 0.10	10.27 ± 0.21	5
k_{off} (min^{-1})[c]	0.037 ± 0.002	0.007 ± 0.001*	3
$t_{1/2}$ (min)[d]	18.7	105	3
k_{on} ($M^{-1}.min^{-1}$)[e]	2.91 ± 0.26 × 10^8	0.90 ± 0.17 × 10^8*	3
Kinetic pK_D[f]	9.93 ± 0.28	10.36 ± 0.22	n.a.

n.a., not applicable, as kinetic pK_D values were calculated from kinetic rate constants k_{on} and k_{off}.

[a]Number of experiments performed for each assay.

[b]Negative logarithm of [^{3}H]NMS equilibrium dissociation constant derived from saturation binding assays.

[c]Dissociation rate constant of [^{3}H]NMS derived from dissociation binding assays.

[d]Half-life dissociation estimate of [^{3}H]NMS calculated from k_{off} estimates.

[e]Association rate constant of [^{3}H]NMS derived from association binding assays.

[f]Negative logarithm of [^{3}H]NMS equilibrium dissociation constant calculated from k_{off}/k_{on}.

*Significantly different from the corresponding value at the wild type ($P < 0.05$), Student's t test.

classic mAChR ligands: ACh, the endogenous ligand for the receptor, and atropine, a classic mAChR orthosteric antagonist. As expected, both ligands completely inhibited the specific binding of [^{3}H]NMS at the WT or the N410K+T423K M_2 mAChR, with both sets of inhibition binding isotherms preferentially fitted (F-test) to a one-site competition binding model (Fig. 2A; Table 2). Although the determined affinity values for both agonist and antagonist at the WT M_2 mAChR were similar to those determined previously by us and others (Valant et al., 2012; Schrage et al., 2014), it was interesting to note that the affinity (pK_I) of each ligand was significantly higher ($P < 0.05$) at the N410K+T423K M_2 mAChR, particularly for the agonist, ACh (Table 2). To determine whether this finding reflected differences in assay conditions between studies (whole cells vs. membranes) and/or properties intrinsic to the mutant receptor, we performed additional membrane-based [^{3}H]NMS binding assays to assess the affinity of ACh in the absence and presence of the nonhydrolyzable guanine nucleotide GppNHp (100 μM; Supplemental Fig. 1). In the absence of nucleotide, ACh displayed a dispersion of high- and low-affinity states at both the wild-type (pK_{HI} = 6.66 ± 0.21; fraction$_{HI}$ = 60%; n = 3; pK_{LO} = 5.06 ± 0.30; n = 3) and the N410K+T423K M_2 mAChRs (pK_{HI} = 7.26 ± 0.16; fraction$_{HI}$ = 57%; n = 3; pK_{LO} = 5.69 ± 0.25; n = 3). In contrast, in the presence of GppNHp, ACh exhibited a single affinity for both wild-type (pK_i = 5.61 ± 0.04; n = 3) and N410K+T423K M_2 mAChRs (pK_i = 6.76 ± 0.09; n = 3) that was, except for the mutant receptor, ~10-fold lower compared with that estimated in intact cells (Table 2). Collectively, these findings suggest that the mutant receptor intrinsically displays a higher affinity for ACh relative to the WT receptor. However, the higher overall affinity observed in whole-cell binding relative to membrane-based assays at this same construct also suggests that an additional mechanism, such as enhanced internalization, is operative in whole-cell assays to yield the higher apparent affinity.

To assess and compare orthosteric ligand functional activity at the N410K+T423K M_2 mAChR, ACh concentration-response curves were constructed to measure both receptor-mediated [^{35}S]GTPγS binding and ERK1/2 phosphorylation. These two pathways were chosen because [^{35}S]GTPγS binding evaluates receptor activation proximally at the level of G protein activation, whereas ERK1/2 phosphorylation is a more downstream response, convergent from multiple pathways

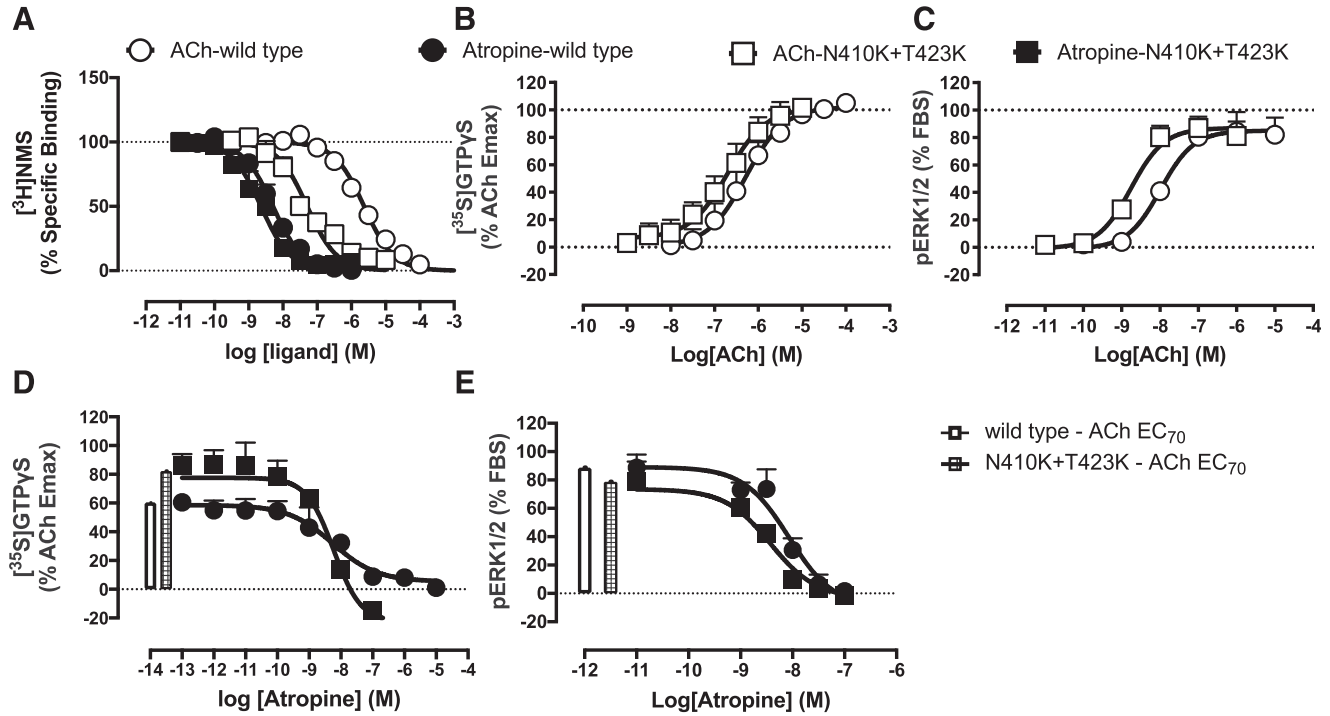

Fig. 2. Binding and functional characterization of orthosteric ligands at the at the wild-type and N410K+T423K M_2 mAChR. (A) [^{3}H]NMS competition binding using atropine or ACh. Functional effects of ACh in [^{35}S]GTPγS binding to activated G proteins (B) or ERK1/2 phosphorylation (pERK1/2) (C). Functional effects of atropine on ACh-mediated [^{35}S]GTPγS binding (D) or pERK1/2 (E). Data points represent the mean ± S.E. obtained from three to five experiments conducted in duplicate.

TABLE 2

Pharmacological parameters of affinity (pK_i or pK_B) and potency (pEC_{50}) of orthosteric ligands at the WT and N410K+T423K M_2 mAChRs

Values represent the mean ± S.E. from at least three experiments performed in duplicate.

Parameters	WT	N410K+T423K	n^a
[^{3}H]NMS binding			
pK_i[b]			
ACh	6.06 ± 0.05	7.71 ± 0.07*	5
Atropine	8.71 ± 0.04	8.96 ± 0.07	5
[^{35}S]GTPγS			
pEC_{50}[c]			
ACh	6.28 ± 0.06	6.70 ± 0.07*	3
pK_B[d]			
Atropine	8.88 ± 0.09	9.00 ± 0.09	3
pERK1/2			
pEC_{50}[c]			
ACh	7.99 ± 0.09	8.76 ± 0.09*	3
pK_B[d]			
Atropine	9.10 ± 0.17	9.38 ± 0.17	3

pERK1/2, phosphorylated ERK1/2.
[a]Number of experiments performed.
[b]Negative logarithm of the orthosteric ligand equilibrium dissociation constant.
[c]Negative logarithm of agonist potency.
[d]Negative logarithm of the orthosteric antagonist equilibrium dissociation constant derived from functional interactions with ACh.
*Significantly different from the corresponding value at the wild type ($P < 0.05$), Student's t test.

with some of them potentially G protein independent. At both the WT and N410K+T423K receptors, the endogenous agonist, ACh, showed robust stimulation of [^{35}S]GTPγS binding and ERK1/2 phosphorylation (Fig. 2, B and C). For both assays, the potencies of ACh at the N410K+T423K M_2 mAChR were significantly higher ($P < 0.05$) than the values obtained using the WT receptor (Table 2). We also evaluated the inhibitory effect of atropine on a fixed (EC_{70}) concentration of ACh in the functional assays at both M_2 mAChR constructs. In contrast to ACh, the estimated functional affinity of atropine for inhibiting agonist signaling in [^{35}S]GTPγS binding and ERK1/2 phosphorylation assay was similar between the WT and the N410K+T423K M_2 mAChRs (Fig. 2, D and E; Table 2).

Effect of the M_2 N410K+T423K Mutation on the Binding Properties of Synthetic Allosteric Modulators. To investigate the effects of mutation of the two key ECV residues on synthetic NAMs of the M_2 mAChR, we performed [^{3}H]NMS equilibrium binding studies using gallamine, arguably the best-characterized NAM of the M_2 mAChR (Clark and Mitchelson, 1976; Dror et al., 2013), as well as two other synthetic M_2 mAChR modulators, strychnine and brucine (Lazareno and Birdsall, 1995; Birdsall et al., 1997; Fig. 3, A and B). Gallamine displayed a near-complete, yet still saturable, inhibition of radioligand binding, indicative of strong negative cooperativity, whereas its effect on [^{3}H]NMS binding at the N410K+T423K M_2 mAChR was virtually abolished compared with the WT receptor. Strychnine and brucine showed a weak enhancement of [^{3}H]NMS binding at the WT receptor, only minimally altering the specific binding of the radioligand at the double-mutant receptor. Application of an allosteric ternary complex model (eq. 3) to the WT M_2 mAChR data provided estimates of the affinity (pK_B) of gallamine, strychnine, and brucine for the unoccupied M_2 mAChR as well as estimates of the cooperativity (α) between the modulators and the radioligand (Table 3). All affinity estimates for the WT receptor were in good agreement with the literature (Lazareno et al., 1998; Dror et al., 2013). Of note, the small effects of synthetic modulators on radioligand binding at the N410K+T423K M_2 mAChR were also quantified, albeit with large

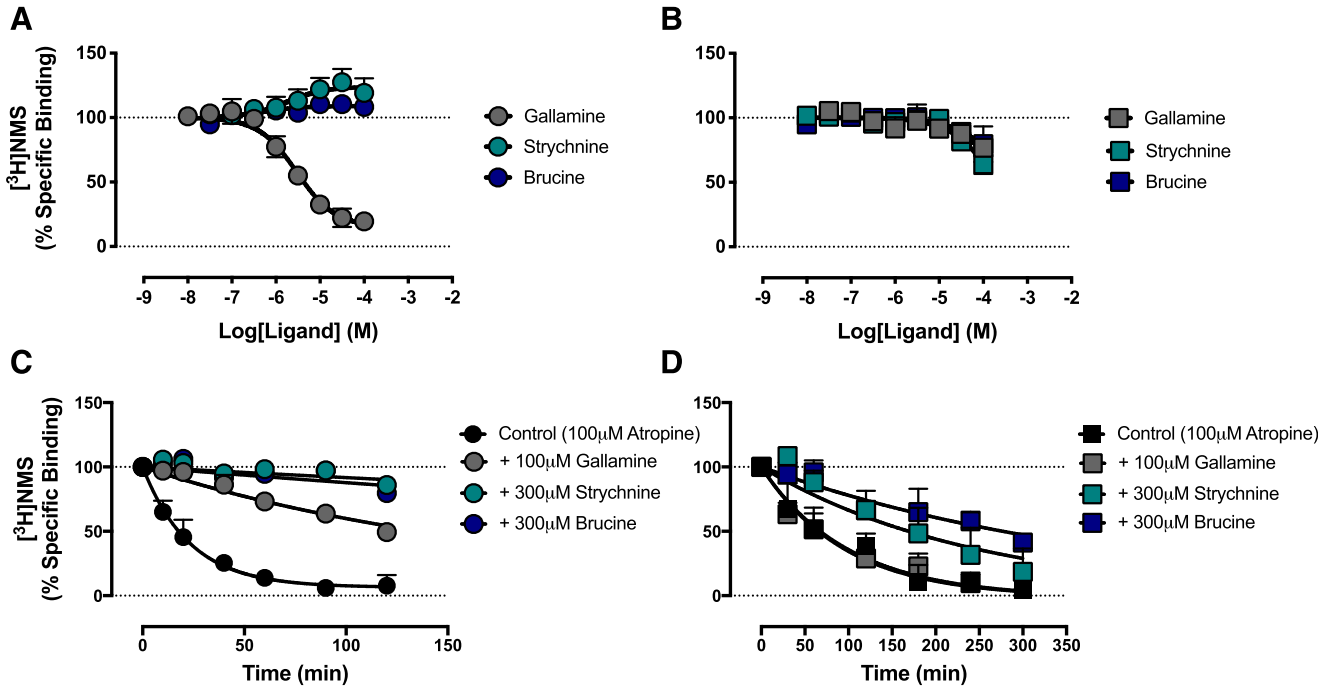

Fig. 3. Binding properties of synthetic small-molecule allosteric modulators at the wild-type and N410K+T423K M_2 mAChR. [^{3}H]NMS equilibrium binding in the presence of increasing concentrations of gallamine, strychnine, or brucine at the wild-type (A) or the N410K+T423K (B) M_2 mAChR. [^{3}H]NMS dissociation in the presence of 100 μM gallamine, 300 μM strychnine, or 300 μM brucine at the wild-type (C) or N410K+T423K (D) M_2 mAChR. Data points represent the mean ± S.E. obtained from three experiments conducted in duplicate.

degrees of error due to the minimal effect exerted. Although the data could be interpreted as either a lack of binding of these synthetic modulators to the "common" allosteric site or a close to neutral cooperativity with the radioligand, the findings nonetheless indicate that the N410K+T423K mutation significantly reduces the allosteric activity of all three synthetic NAMs.

To investigate the effects of the M_2 mAChR mutations on the ability of synthetic modulators to affect [^{3}H]NMS dissociation, we then determined the radioligand k_{off} in the absence or presence of a high concentration of each modulator and compared these effects to the WT M_2 mAChR. As shown in Fig. 3C, the synthetic allosteric compounds caused a significant retardation in [^{3}H]NMS dissociation compared with the control dissociation rate, consistent with their ability to bind the ECV region and thus prevent egress of the radioligand out of the orthosteric site. In contrast, when these experiments were repeated at the N410K+T423K M_2 mAChR, the ability of the modulators to retard radioligand dissociation was significantly reduced, an effect that was most pronounced for gallamine (Fig. 3D; Table 3).

Effect of the M_2 N410K+T423K Mutation on the Functional Properties of Synthetic Allosteric Modulators. Using a similar protocol as described earlier (Fig. 2D) for the [^{35}S]GTPγS binding assay, we determined the pharmacological properties of the three prototypical modulators against ACh responses at both the WT and the N410K+T423K M_2 mAChRs. In contrast to their effects on [^{3}H]NMS binding, all three allosteric ligands exhibited NAM activity against ACh-mediated signaling at the WT receptor (Fig. 4, A, C, and E). Strikingly, gallamine, strychnine, and brucine displayed significantly reduced effects on ACh-mediated responses at the N410K+T423K M_2 mAChR (Fig. 4, B, D, and F). Application of an allosteric ternary complex model (eq. 6) to the data allowed us to derive estimates of both the functional affinity of each modulator and its cooperativity with ACh (Table 4). Collectively, these findings indicate that the two rationally designed mutations (N410K+T423K) at the top of transmembrane 6 (TM6) and TM7 in the M_2 mAChR play a major role in prototypical NAM activity, both at the level of binding and function, thus validating the N410K+T423K M_2 mAChR as an allosteric site-impaired receptor, at least with respect to modulators that interact with the "common" allosteric site located in the ECV.

Use of the Allosteric Site-Impaired M_2 mAChR to Validate an Allosteric Mode of Action of Positively Charged Basic Proteins. A number of highly basic, arginine-rich proteins, including MBP, have been suggested to interact allosterically with [^{3}H]NMS at the M_2 mAChR (Hu et al., 1992; Hu and el-Fakahany, 1993; Fryer and Jacoby, 1998). MBP is toxic for parasites and pathogens, such that its cytotoxicity is key to its mechanism of defense in asthma attacks (Jacoby et al., 1993). In an attempt to assess its toxicity, we measured the spontaneous release of LDH in the presence of MBP on intact CHO cells (Supplemental Fig. 1). MBP did not affect cell integrity at 1 μM but did indeed induce spontaneous LDH release at 3 μM. Avoiding concentrations that induced MBP-driven cytotoxicity, we then assessed the pharmacological properties of three peptides [MBP, protamine, and poly-L-arginine (PLA)] on M_2 mAChR CHO cells. As shown in Fig. 5A, increasing concentrations of the PLA and protamine resulted in a near-complete inhibition of radioligand binding to the M_2 mAChR, whereas MBP did not appear to alter the specific binding of the radioligand at concentrations up to 1 μM. Application of an allosteric ternary complex model (eq. 3) to these data allowed us to derive affinity estimates for PLA and protamine for the unoccupied receptor (pK_B) and their cooperativity with the radioligand (logα_{NMS}) (Table 5). Of note, the near-complete inhibition of radioligand binding by protamine and PLA could suggest either a competitive interaction or a negative allosteric effect characterized by very high negative cooperativity. Irrespective, under this latter condition, the affinity estimate derived from an allosteric model with high negative cooperativity (Table 5) would be indistinguishable from that estimated using a simple competitive model (Keov et al., 2014), thus the pK_B estimates for the ligands remain valid. In an effort to more-directly confirm an allosteric mode of binding for peptide modulators, we also performed dissociation kinetic experiments using [^{3}H]NMS and the highest concentrations of two of our selected basic peptides that could be used experimentally based on physicochemical properties and compound availability, which were 10 μM for PLA and 30 μM for protamine (Fig. 5C). For protamine and PLA, these concentrations were ~10× higher than their K_B concentrations and caused a small but significant effect on radioligand dissociation (Fig. 5C; Table 5). Because the interaction of each substance with [^{3}H]NMS is characterized by negative cooperativity, it is not surprising that substantial effects on radioligand dissociation were not observed

TABLE 3

Allosteric parameter estimates for gallamine, strychnine, and brucine at the WT and N410K+T423K M_2 mAChRs

Values represent the mean ± S.E. from at least three experiments performed in duplicate.

	WT					N410K+T423K				
	pK_B[a]	Logα_{NMS}[b]	n[c]	k_{off} (min^{-1})[d]	n[c]	pK_B	Logα_{NMS}	n	k_{off} (min^{-1})	n
Gallamine	5.98 ± 0.05	−1.15 ± 0.05	6	0.0056 ± 0.0003^	4	3.91 ± 0.20*	−0.57 ± 0.11	3	0.010 ± 0.002	3
Strychnine	5.48 ± 0.30	0.38 ± 0.06	3	0.0009 ± 0.0002^	3	n.a	n.a	4	0.004 ± 0.001	3
Brucine	5.58 ± 0.34	0.14 ± 0.03	3	0.0014 ± 0.0003^	3	4.34 ± 0.34*	−0.36 ± 0.18	4	0.002 ± 0.001	3

n.a., not applicable, as no alteration of the specific binding of the radioligand was observed, and therefore, no estimate could be provided.

[a]Negative logarithm of the allosteric modulator equilibrium dissociation constant.

[b]Logarithm of the cooperativity factor for the interaction between the modulators and the orthosteric radioligand.

[c]Number of experiments performed.

[d]Dissociation rate constant of the [^{3}H]NMS in the presence of the indicated ligand (control values in the absence of ligand: WT k_{off} = 0.043 ± 0.003 min^{-1}, N410K+T423K mutant k_{off} = 0.007 ± 0.001 min^{-1}).

*Significantly different from the corresponding value at the wild type ($P < 0.05$), Student's t test.

^Significantly different from k_{off} with 100 μM atropine only ($P < 0.05$), one-way analysis of variance with Dunnett's post-test.

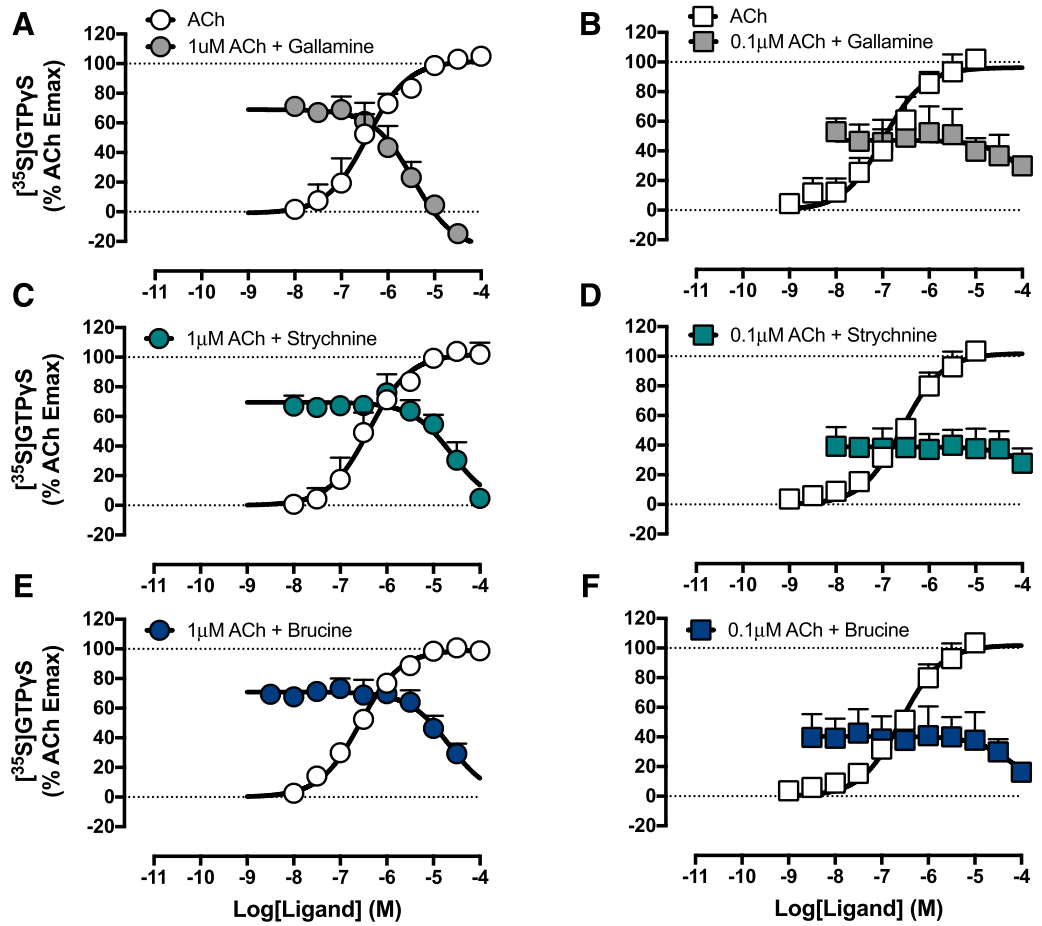

Fig. 4. Functional effects of synthetic small-molecule allosteric modulators at the wild-type and N410K+T423K M_2 mAChR. Effect of gallamine on EC_{70} concentration of ACh at the wild-type (A) or N410K+T423K (B) M_2 mAChR. Effect of strychnine on EC_{70} concentration of ACh at the wild-type (C) or N410K+T423K (D) M_2 mAChR. Effect of brucine on EC_{70} concentration of ACh at the wild-type (E) or N410K+T423K (F) M_2 mAChR. Data points represent the mean ± S.E. obtained from three experiments conducted in duplicate.

since the receptor is pre-equilibrated with [^{3}H]NMS and thus would require much higher concentrations of the peptides than can be attained experimentally to ensure substantial allosteric site occupancy to overcome the negative cooperativity (Lane et al., 2017). MBP was not tested, as the experimental protocol required a too-large amount of protein.

Such results from equilibrium binding and dissociation kinetic experiments highlight an inherent difficulty in differentiating allosteric modulators that exhibit high negative cooperativity from orthosteric (competitive) antagonists. In this context, our novel allosteric site-impaired M_2 mAChR can prove a useful alternative. Thus, we determined the pharmacological properties of PLA, MBP, and protamine at this construct. In [^{3}H]NMS equilibrium binding assays using the N410K+T423K M_2 mAChR, the effect of each peptide on [^{3}H]NMS was substantially blunted compared with the WT (Fig. 5B; Table 5). Specifically, and in accordance with the structure-based design of the mutant receptor, the affinity of each cationic peptide for the allosteric site was significantly reduced compared with the WT ($P < 0.05$), with MBP remaining neutral (Table 5). In addition, a dramatic loss of cooperativity with the radioligand was observed for PLA. Moreover, in [^{3}H]NMS dissociation kinetic assays at the N410K+T423K M_2 mAChR, neither PLA nor protamine had any effect on [^{3}H]NMS dissociation (Fig. 5D; Table 5) due to a lack of sufficient allosteric site occupancy at the maximal concentrations attainable in this assay.

Excitingly, when we investigated the allosteric properties of the basic, arginine-rich peptides in assays of M_2 mAChR function, we found the allosteric effects of all peptides

TABLE 4

Affinity (pK_B) and functional cooperativity with ACh ($\log\alpha\beta_{ACh}$) estimates of the prototypical NAMs in [^{35}S]GTPγS binding accumulation assay at the wild-type and N410K+T423K M_2 mAChRs

Values represent the mean ± S.E. from at least three experiments performed in duplicate.

	WT			N410K+T423K		
	pK_B[a]	$\log\alpha\beta_{ACh}$[b]	n[c]	pK_B[a]	$\log\alpha\beta_{ACh}$[b]	n
Gallamine	6.08 ± 0.16	−3[#]	3	4.12 ± 0.21*	−3[#]	4
Strychnine	5.13 ± 0.05	−3[#]	3	3.55 ± 0.36*	−3[#]	4
Brucine	5.42 ± 0.14	−3[#]	3	4.21 ± 0.22*	−3[#]	4

[a]Negative logarithm of the allosteric modulator equilibrium dissociation constant.
[b]Logarithm of the functional cooperativity for the interaction between the modulator and ACh; in all instances, the interaction was indistinguishable from competition (F-test), indicative of very high negative cooperativity ($\alpha\beta \to 0$), and thus cooperativity values were constrained to an arbitrarily low value, #.
[c]Number of experiments performed.
*Significantly different from the corresponding value at the wild type ($P < 0.05$), Student's t test.
[#]Arbitrarily low value.

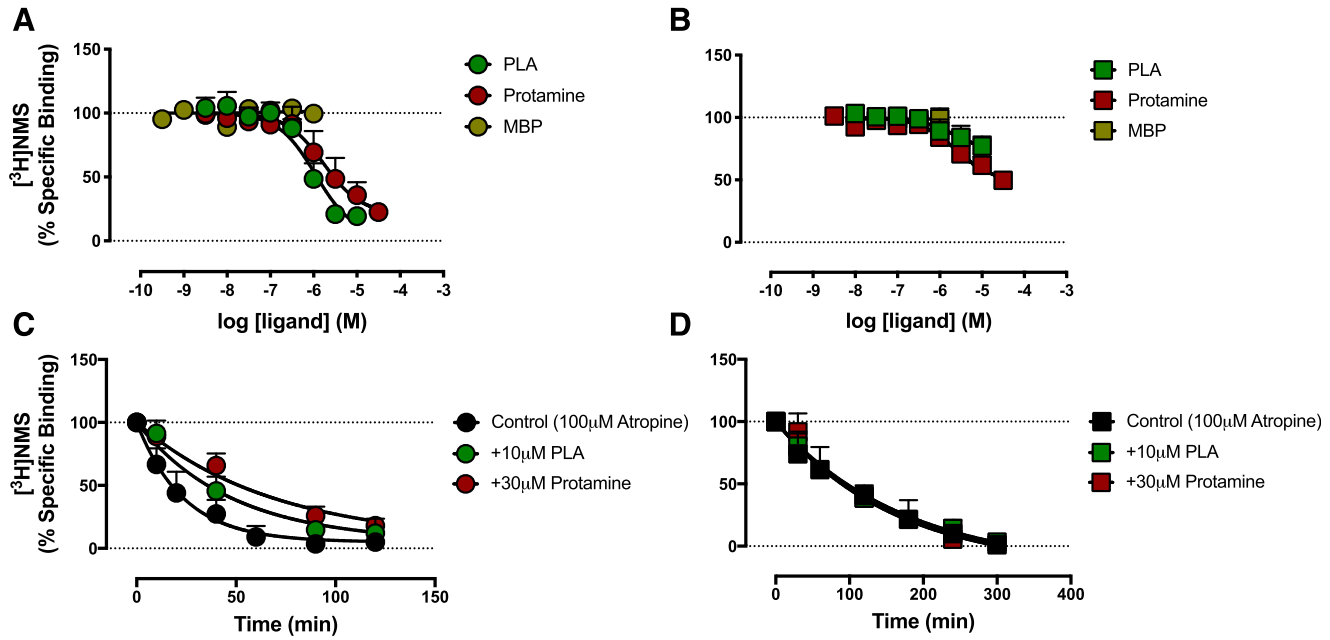

Fig. 5. Validation of allosteric interaction between [^{3}H]NMS and cationic peptide modulators at the wild-type and N410K+T423K M_2 mAChR. [^{3}H]NMS interaction with PLA, protamine, and MBP at the wild-type (A) or the N410K+T423K (B) M_2 mAChR. [^{3}H]NMS dissociation in the presence of a single high concentration of PLA, protamine, or MBP at the wild-type (C) or N410K+T423K (D) M_2 mAChR. Data points represent the mean ± S.E. obtained from three experiments conducted in duplicate.

substantially altered ACh-mediated responses in the [^{35}S]GTPγS assay, including MBP (Fig. 6). At the WT M_2 mAChR, all three peptides inhibited the response produce by a fixed concentration of ACh in a concentration-dependent manner (Fig. 6, A, C, and E). These findings validate our previous observation in radioligand binding for PLA and protamine but also suggest that MBP can bind the M_2 mAChR with an NAM effect on the endogenous ligand, albeit with an neutral allosteric ligand effect on the antagonist radioligand. At the allosteric site-impaired M_2 mAChR, these effects were significantly reduced (Fig. 6, B, D, and F), consistent with the hypothesis that mutation of N410 and T423 to lysine blunts the pharmacological effects of cationic NAMs (Table 6). Taken together, our data at the N410K+T423K M_2 mAChR suggest that these two point mutations abrogate the activity of cationic NAMs at the M_2 mAChR and validate structure-based approaches for understanding GPCR allosteric binding sites with regard to both synthetic and putative endogenous modulators.

Discussion

Recently, we used a structure-based approach to design a mutant M_2 mAChR (N410K+T423K) that, in preliminary studies, substantially reduced the binding of two synthetic cationic NAMs of the M_2 mAChR, gallamine and heptane-1,7-bis(dimethyl-3′phthalimodipropylammonium) (Dror et al., 2013). Given the location of the mutations in the key ECV that contains a well characterized common allosteric site in the mAChR family and the abundance of structurally diverse cationic modulators for these receptors, the current study investigated and characterized the pharmacological properties of this putative allosteric site-impaired receptor. Based on our results, we propose that this mutant M_2 mAChR can be used as a novel construct to validate the allosteric mode of

TABLE 5

Allosteric parameters of affinity (pK_B), binding cooperativity ($\log\alpha_{NMS}$) of basic peptides, and [^{3}H]NMS dissociation rate (k_{off}) at the wild type

Values represent the mean ± S.E. from at least three experiments performed in duplicate.

	WT					N410K+T423K				
	pK_B[a]	$\log\alpha_{NMS}$[b]	n[c]	k_{off} (min^{-1})[d]	n	pK_B[a]	$\log\alpha_{NMS}$[b]	n	k_{off} (min^{-1})[c]	n
PLA	6.32 ± 0.08	−1.51 ± 0.22	4	0.021 ± 0.002^	3	5.76 ± 0.20*	−0.19 ± 0.03*	3	0.006 ± 0.001	3
MBP	n.a.	n.a.	4	n.t.	n.t.	n.a.	n.a.	4	n.t.	n.t.
Protamine	6.08 ± 0.09	−1.08 ± 0.10	3	0.014 ± 0.002^	3	5.46 ± 0.12*	−0.79 ± 0.15*	5	0.006 ± 0.001	3

n.a., not applicable, as no alteration of the specific binding of the radioligand was observed, and therefore, no estimate could be provided; n.t., not tested.

[a]Negative logarithm of the allosteric modulator equilibrium dissociation constant.

[b]Logarithm of the cooperativity factor for the interaction between the peptides and [^{3}H]NMS.

[c]Number of experiments performed.

[d]Dissociation rate constant of the [^{3}H]NMS in the presence of the indicated ligand (control values in the absence of ligand: WT k_{off} = 0.043 ± 0.003 min^{-1}, N410K+T423K k_{off} = 0.007 ± 0.001 min^{-1}).

*Significantly different from the corresponding value at the wild type ($P < 0.05$), Student's t test.

^Significantly different from control k_{off} ($P < 0.05$), one-way analysis of variance with Dunnett's post-test.

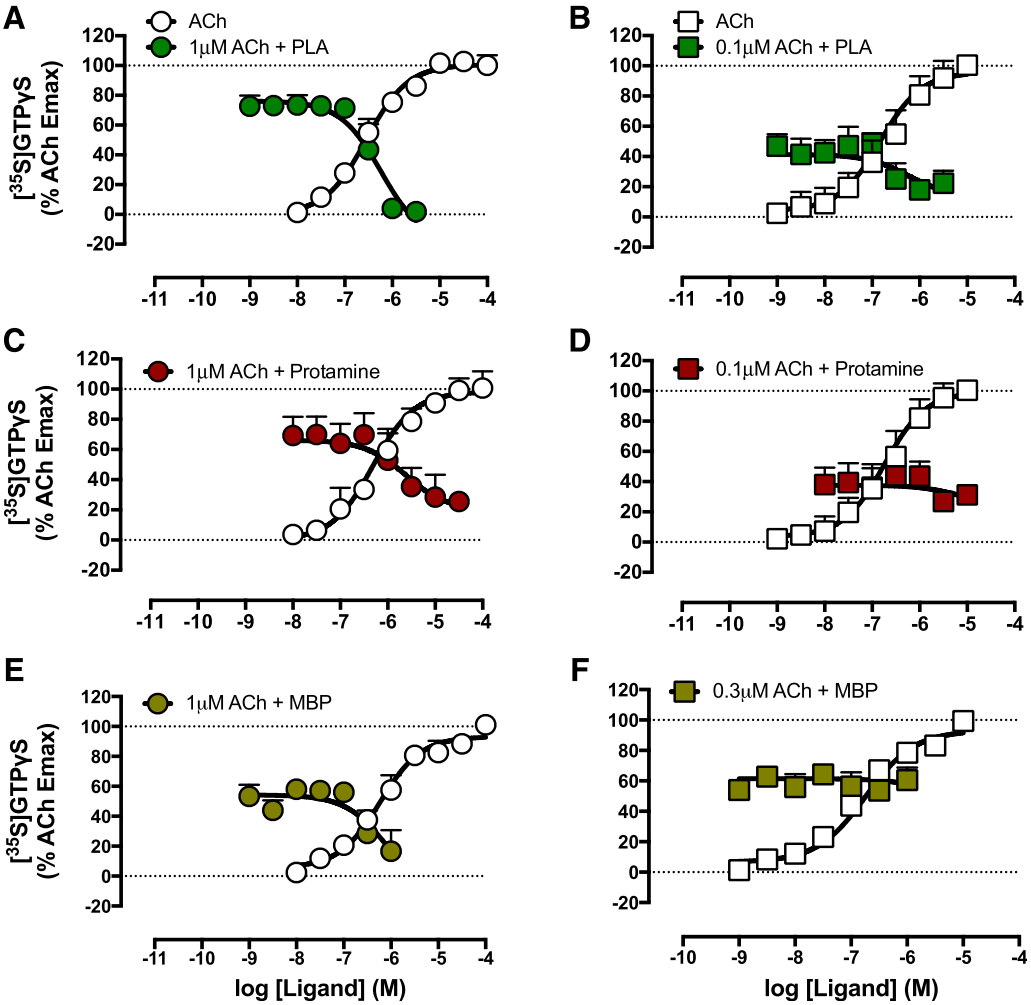

Fig. 6. Functional effects of cationic peptide modulators at the wild-type and N410K+T423K M_2 mAChR. Effect of poly-L-arginine on EC_{70} concentration of ACh at the wild-type (A) or N410K+T423K (B) M_2 mAChR. Effect of protamine on EC_{70} concentration of ACh at the wild-type (C) or N410K+T423K (D) M_2 mAChR. Effect of MBP on EC_{70} concentration of ACh at the wild-type (E) or N410K+T423K (F) M_2 mAChR. Data points represent the mean ± S.E. obtained from three experiments conducted in duplicate.

action of subtype-selective cationic NAMs displaying high degrees of negative cooperativity with orthosteric ligands. Moreover, we used this mutant receptor to provide further evidence in support of a potential allosteric mode of action of positively charged peptides, including the endogenously produced protamine and MBP.

A hallmark of allosteric drugs that modulate orthosteric ligand affinity is their ability to change orthosteric ligand association and/or dissociation rates to achieve such affinity modulation (Lane et al., 2017). Traditionally, dissociation kinetic studies are the preferred means for validating such allosteric effects, since the observed association of a labeled

TABLE 6

Affinity (pK_B) and functional cooperativity with ACh ($\log\alpha\beta_{ACh}$) estimates of the basic peptides, PLA, protamine, and MBP

Values represent the mean ± S.E. from at least three experiments performed in duplicate.

	WT			N410K+T423K		
	pK_B[a]	$\text{Log}\alpha\beta_{ACh}$[b]	n[c]	pK_B	$\text{Log}\alpha\beta_{ACh}$	n
PLA	7.00 ± 0.05	−3[#]	3	6.41 ± 0.25*	−0.70 ± 0.56*	3
MBP	6.54 ± 0.29	−3[#]	4	n.a.	n.a.	4
Protamine	6.01 ± 0.25	−0.86 ± 0.19	4	n.a.	n.a.	4

n.a., not applicable, as no alteration of the EC_{50} of ACh was observed, and therefore, no estimate could be provided.
[a]Negative logarithm of the allosteric modulator equilibrium dissociation constant.
[b]Logarithm of the cooperativity factor for the interaction between the peptides and ACh.
[c]Number of experiments performed.
*Significantly different from the corresponding value at the wild type ($P < 0.05$), Student's t test.
[#]Interaction was indistinguishable from competition (F-test), indicative of very high negative cooperativity ($\alpha\beta \rightarrow 0$), and thus the cooperativity factor was constrained to an arbitrarily low value.

orthosteric ligand can still be reduced in the presence of a second orthosteric (competitive) ligand due to simple mass action as the system approaches equilibrium. In contrast, the only way that dissociation of a prelabeled receptor-ligand complex can be modified is through a conformational change via the binding of a second ligand at a spatially distinct site (Lane et al., 2017). Unfortunately, due to the reciprocal nature of allosteric interactions, NAMs exhibiting high negative cooperativity with orthosteric ligands will themselves have a markedly reduced affinity for the radioligand-occupied receptor, necessitating extremely high concentrations ($\sim 100 \times K_B$) to ensure sufficient allosteric site occupancy to observe a significant effect on radioligand k_{off}. Similar considerations apply to the study of NAMs in equilibrium binding assays, where high negative cooperativity may be indistinguishable from a competitive interaction. In all such instances, high concentrations of interacting ligands are invariably required to differentiate allosteric from orthosteric mechanisms, which is not feasible for compounds that possess low affinity for the receptor and/or unfavorable physicochemical properties. This question is particularly relevant for previously identified basic, arginine-rich, endogenous peptides that have been suggested to potentially target the M_2 mAChR in an allosteric fashion (Hu et al., 1992; Hu and el-Fakahany, 1993; Fryer and Jacoby, 1998), such that an unambiguous validation of an allosteric mode of binding using traditional approaches is difficult. In that situation, the use of a rationally designed allosteric site-impaired receptor may overcome the limitations associated with classic approaches.

Another interesting observation at the allosteric site-impaired receptor was that it exhibited a small, albeit significant, increased affinity for the endogenous orthosteric agonist, ACh. Ligand affinity is dependent on the ratio of dissociation (k_{off}) and association (k_{on}) rate constants, and it is likely that the increased affinity of ACh at the allosteric site-impaired receptor reflects a change in either (or both) of these parameters compared with the WT. This is consistent with the suggestion that the two mutated residues are involved in orthosteric ligand access to and egress from its pocket, which sits below the ECV within the TM bundle. In fact, by comparing the change of [^{3}H]NMS association and dissociation rates in the WT and N410K+T423K M_2 mAChRs, we observed a significant reduction in both the k_{on} and k_{off} rates, albeit to similar extents such that equilibrium affinity was largely unaffected. In contrast, it is possible that the increased affinity observed for ACh indicates a change to a different extent between the k_{on} and/or the k_{off} of the endogenous ligand, and that agonists are perhaps more susceptible to changes in these ECV residues than antagonists such as NMS or atropine. It is known that mutations within a GPCR, even outside the orthosteric binding site, can dramatically change the kinetic parameters of orthosteric ligands (Matsui et al., 1995; Dror et al., 2013). In fact, it has been demonstrated previously that orthosteric ligands of some class A GPCRs adopt a transient metastable pose in the extracellular regions of the receptor prior to transit to the orthosteric site (Redka et al., 2008; Dror et al., 2011, 2013; Nguyen et al., 2016). Thus, it is not surprising that mutations within an allosteric ECV may indirectly alter orthosteric ligand affinity through changes in kinetic properties. Indeed, some mAChR orthosteric antagonists that have yielded positive clinical results in the treatment of chronic obstructive pulmonary disease specifically exploit differences in kinetic rates between mAChR family members as part of their proposed mechanism of action (Sykes et al., 2012; Tautermann et al., 2013). For example, while exhibiting fast dissociation from the M_2 mAChR, glycopyrrolate remains bound approximately 10 times longer at the M_3 mAChR orthosteric site due to a slower k_{off}, exhibiting what has been termed "kinetic selectivity" (Tautermann et al., 2013). This difference in kinetic rates between the two mAChR subtypes is likely a consequence of the presence of nonconserved amino acid residues in the ECV. Moreover, comparison of the ECV of the M_2 with the M_3 mAChR shows clear differences in electrostatic surface potentials (Thal et al., 2016), which can also contribute to differences in kinetic rate constants of both orthosteric and allosteric ligands that interact with these receptors.

Arguably, however, the most important findings through the use of the ECV mutant M_2 mAChR relate to the effects noted on both small-molecule and peptide/protein allosteric modulators, whereby the introduction of positively charged residues in the ECV of the M_2 mAChR significantly altered the affinity of all allosteric modulators, suggesting that this charge effect is a common mechanism. In addition, the mutation also affected the cooperativity between some of the modulators and orthosteric ligands, suggesting additional dynamic mechanisms that may be ligand-specific. Given the rational design of the mutant to promote electrostatic charge-charge repulsion between cationic substances and the two key allosteric site residues, it is not surprising that the most marked effect was noted with gallamine, which is a small synthetic molecule that possesses three positive charges, when interacting with the M_2 mAChR; electrostatic repulsion between gallamine and the positively charged [^{3}H]NMS at the wild-type M_2 mAChR has even been proposed as the major mechanism underlying the observed negative cooperativity between the two ligands (Dror et al., 2013). In addition, the significant effects noted on the binding of the additional synthetic modulators, strychnine and brucine, which have both been previously proposed to interact via the common ECV allosteric site (Jakubík et al., 2005), also highlight the key role of the mutated residues in the binding of prototypical modulators regardless of their scaffold. In contrast, the reduction in affinities and/or cooperativities for the cationic peptides was relatively more modest but nonetheless significant. On the one hand, the abrogation in the effects of protamine and MBP, which are both produced endogenously, provides further support for a relatively unappreciated role of these substances as putative endogenous allosteric ligands and thus warrants further study. On the other hand, the stronger effects on the synthetic small molecules relative to the larger peptides/proteins suggest that electronegativity in the ECV, although important, is unlikely to be the sole required feature for basic peptidic modulators to bind allosterically at the M_2 mAChR. PLA, MBP, and protamine are very large entities and, therefore, can anchor themselves via multiple points of interaction, rendering them perhaps less sensitive to the change in electronegativity from only two residues.

Nonetheless, this study validated a novel molecular construct for assessing and validating allosteric binding modes for both synthetic and putative endogenous modulators that exhibit high negative cooperativity through interaction with the ECV of the M_2 mAChR. In addition to affecting modulator

binding, this allosteric site-impaired M_2 mAChR also has additional effects on the cooperativity of some of the synthetic and basic arginine-rich peptides, suggesting some commonalities in their mode of interaction with the receptor. Structure-based design of such mutant receptors thus represents a valuable new strategy for assisting drug discovery and chemical biology studies of GPCR allostery. Although speculative, the allosteric site-impaired M_2 mAChR may also prove a new candidate for future chemogenetic strategies, such as through the generation of transgenic models that can be used to understand the potential physiologic relevance of endogenous cationic modulators of this GPCR.

Authorship Contributions

Participated in research design: Moo, Christopoulos, Valant.

Conducted experiments: Moo, Valant.

Performed data analysis: Moo, Valant.

Wrote or contributed to the writing of the manuscript: Moo, Sexton, Christopoulos, Valant.

References

Abrams P, Andersson KE, Buccafusco JJ, Chapple C, de Groat WC, Fryer AD, Kay G, Laties A, Nathanson NM, Pasricha PJ, et al. (2006) Muscarinic receptors: their distribution and function in body systems, and the implications for treating overactive bladder. *Br J Pharmacol* **148**:565–578.

Ackerman SJ, Loegering DA, Venge P, Olsson I, Harley JB, Fauci AS, and Gleich GJ (1983) Distinctive cationic proteins of the human eosinophil granule: major basic protein, eosinophil cationic protein, and eosinophil-derived neurotoxin. *J Immunol* **131**:2977–2982.

Birdsall NJ, Farries T, Gharagozloo P, Kobayashi S, Kuonen D, Lazareno S, Popham A, and Sugimoto M (1997) Selective allosteric enhancement of the binding and actions of acetylcholine at muscarinic receptor subtypes. *Life Sci* **60**:1047–1052.

Caulfield MP and Birdsall NJ (1998) International Union of Pharmacology. XVII. Classification of muscarinic acetylcholine receptors. *Pharmacol Rev* **50**:279–290.

Changeux JP and Christopoulos A (2016) Allosteric modulation as a unifying mechanism for receptor function and regulation. *Cell* **166**:1084–1102.

Cheng Y and Prusoff WH (1973) Relationship between the inhibition constant (K1) and the concentration of inhibitor which causes 50 per cent inhibition (I50) of an enzymatic reaction. *Biochem Pharmacol* **22**:3099–3108.

Christopoulos A (1998) Assessing the distribution of parameters in models of ligand-receptor interaction: to log or not to log. *Trends Pharmacol Sci* **19**:351–357.

Christopoulos A (2002) Allosteric binding sites on cell-surface receptors: novel targets for drug discovery. *Nat Rev Drug Discov* **1**:198–210.

Christopoulos A and Kenakin T (2002) G protein-coupled receptor allosterism and complexing. *Pharmacol Rev* **54**:323–374.

Christopoulos A, Lanzafame A, and Mitchelson F (1998) Allosteric interactions at muscarinic cholinoceptors. *Clin Exp Pharmacol Physiol* **25**:185–194.

Clark AL and Mitchelson F (1976) The inhibitory effect of gallamine on muscarinic receptors. *Br J Pharmacol* **58**:323–331.

Draper-Joyce CJ, Michino M, Verma RK, Klein Herenbrink C, Shonberg J, Kopinathan A, Scammells PJ, Capuano B, Thal DM, Javitch JA, et al. (2018) The structural determinants of the bitopic binding mode of a negative allosteric modulator of the dopamine D_2 receptor. *Biochem Pharmacol* **148**: 315–328.

Dror RO, Green HF, Valant C, Borhani DW, Valcourt JR, Pan AC, Arlow DH, Canals M, Lane JR, Rahmani R, et al. (2013) Structural basis for modulation of a G-protein-coupled receptor by allosteric drugs. *Nature* **503**:295–299.

Dror RO, Pan AC, Arlow DH, Borhani DW, Maragakis P, Shan Y, Xu H, and Shaw DE (2011) Pathway and mechanism of drug binding to G-protein-coupled receptor. *Proc Natl Acad Sci USA* **108**:13118–13123.

Fryer AD and Jacoby DB (1998) Muscarinic receptors and control of airway smooth muscle. *Am J Respir Crit Care Med* **158**:S154–S160.

Gregory KJ, Hall NE, Tobin AB, Sexton PM, and Christopoulos A (2010) Identification of orthosteric and allosteric site mutations in M2 muscarinic acetylcholine receptors that contribute to ligand-selective signaling bias. *J Biol Chem* **285**: 7459–7474.

Gregory KJ, Sexton PM, and Christopoulos A (2007) Allosteric modulation of muscarinic acetylcholine receptors. *Curr Neuropharmacol* **5**:157–167.

Haga K, Kruse AC, Asada H, Yurugi-Kobayashi T, Shiroishi M, Zhang C, Weis WI, Okada T, Kobilka BK, Haga T, et al. (2012) Structure of the human M2 muscarinic acetylcholine receptor bound to an antagonist. *Nature* **482**:547–551.

Hu J and el-Fakahany EE (1993) Allosteric interaction of dynorphin and myelin basic protein with muscarinic receptors. *Pharmacology* **47**:351–359.

Hu J, Wang SZ, Forray C, and el-Fakahany EE (1992) Complex allosteric modulation of cardiac muscarinic receptors by protamine: potential model for putative endogenous ligands. *Mol Pharmacol* **42**:311–321.

Jacoby DB, Gleich GJ, and Fryer AD (1993) Human eosinophil major basic protein is an endogenous allosteric antagonist at the inhibitory muscarinic M2 receptor. *J Clin Invest* **91**:1314–1318.

Jakubík J, Krejcí A, and Dolezal V (2005) Asparagine, valine, and threonine in the third extracellular loop of muscarinic receptor have essential roles in the positive cooperativity of strychnine-like allosteric modulators. *J Pharmacol Exp Ther* **313**: 688–696.

Keov P, López L, Devine SM, Valant C, Lane JR, Scammells PJ, Sexton PM, and Christopoulos A (2014) Molecular mechanisms of bitopic ligand engagement with the M1 muscarinic acetylcholine receptor. *J Biol Chem* **289**:23817–23837.

Kruse AC, Hu J, Pan AC, Arlow DH, Rosenbaum DM, Rosemond E, Green HF, Liu T, Chae PS, Dror RO, et al. (2012) Structure and dynamics of the M3 muscarinic acetylcholine receptor. *Nature* **482**:552–556.

Kruse AC, Kobilka BK, Gautam D, Sexton PM, Christopoulos A, and Wess J (2014) Muscarinic acetylcholine receptors: novel opportunities for drug development. *Nat Rev Drug Discov* **13**:549–560.

Kruse AC, Ring AM, Manglik A, Hu J, Hu K, Eitel K, Hübner H, Pardon E, Valant C, Sexton PM, et al. (2013) Activation and allosteric modulation of a muscarinic acetylcholine receptor. *Nature* **504**:101–106.

Lane JR, May LT, Parton RG, Sexton PM, and Christopoulos A (2017) A kinetic view of GPCR allostery and biased agonism. *Nat Chem Biol* **13**:929–937.

Langmead CJ, Watson J, and Reavill C (2008) Muscarinic acetylcholine receptors as CNS drug targets. *Pharmacol Ther* **117**:232–243.

Lazareno S and Birdsall NJ (1995) Detection, quantitation, and verification of allosteric interactions of agents with labeled and unlabeled ligands at G protein-coupled receptors: interactions of strychnine and acetylcholine at muscarinic receptors. *Mol Pharmacol* **48**:362–378.

Lazareno S, Gharagozloo P, Kuonen D, Popham A, and Birdsall NJM (1998) Subtype-selective positive cooperative interactions between brucine analogues and acetylcholine at muscarinic receptors: radioligand binding studies. *Mol Pharm* **53**: 573–589.

Matsui H, Lazareno S, and Birdsall NJ (1995) Probing of the location of the allosteric site on m1 muscarinic receptors by site-directed mutagenesis. *Mol Pharmacol* **47**: 88–98.

May LT, Leach K, Sexton PM, and Christopoulos A (2007) Allosteric modulation of G protein-coupled receptors. *Annu Rev Pharmacol Toxicol* **47**:1–51.

Nguyen ATN, Baltos J-A, Thomas T, Nguyen TD, Muñoz LL, Gregory KJ, White PJ, Sexton PM, Christopoulos A, and May LT (2016) Extracellular loop 2 of the adenosine A_1 receptor has a key role in orthosteric ligand affinity and agonist efficacy. *Mol Pharmacol* **90**:703–714.

Redka DS, Pisterzi LF, and Wells JW (2008) Binding of orthosteric ligands to the allosteric site of the M(2) muscarinic cholinergic receptor. *Mol Pharmacol* **74**: 834–843.

Santos R, Ursu O, Gaulton A, Bento AP, Donadi RS, Bologa CG, Karlsson A, Al-Lazikani B, Hersey A, Oprea TI, et al. (2017) A comprehensive map of molecular drug targets. *Nat Rev Drug Discov* **16**:19–34.

Schrage R, Holze J, Klöckner J, Balkow A, Klause AS, Schmitz A-L, De Amici M, Kostenis E, Tränkle C, Holzgrabe U, et al. (2014) New insight into active muscarinic receptors with the novel radioagonist [^{3}H]iperoxo. *Biochem Pharmacol* **90**: 307–319.

Sykes DA, Dowling MR, Leighton-Davies J, Kent TC, Fawcett L, Renard E, Trifilieff A, and Charlton SJ (2012) The Influence of receptor kinetics on the onset and duration of action and the therapeutic index of NVA237 and tiotropium. *J Pharmacol Exp Ther* **343**:520–528.

Tautermann CS, Kiechle T, Seeliger D, Diehl S, Wex E, Banholzer R, Gantner F, Pieper MP, and Casarosa P (2013) Molecular basis for the long duration of action and kinetic selectivity of tiotropium for the muscarinic M3 receptor. *J Med Chem* **56**:8746–8756.

Thal DM, Sun B, Feng D, Nawaratne V, Leach K, Felder CC, Bures MG, Evans DA, Weis WI, Bachhawat P, et al. (2016) Crystal structures of the M1 and M4 muscarinic acetylcholine receptors. *Nature* **531**:335–340.

Valant C, Felder CC, Sexton PM, and Christopoulos A (2012) Probe dependence in the allosteric modulation of a G protein-coupled receptor: implications for detection and validation of allosteric ligand effects. *Mol Pharmacol* **81**:41–52.

van der Westhuizen ET, Valant C, Sexton PM, and Christopoulos A (2015) Endogenous allosteric modulators of G protein-coupled receptors. *J Pharmacol Exp Ther* **353**:246–260.

Wess J, Eglen RM, and Gautam D (2007) Muscarinic acetylcholine receptors: mutant mice provide new insights for drug development. *Nat Rev Drug Discov* **6**:721–733.

Address correspondence to: Arthur Christopoulos, Drug Discovery Biology and Department of Pharmacology, Monash Institute of Pharmaceutical Sciences, Monash University, 399 Royal Parade, Parkville VIC 3052, Australia. E-mail: arthur.christopoulos@monash.edu; or Celine Valant, Drug Discovery Biology and Department of Pharmacology, Monash Institute of Pharmaceutical Sciences, Monash University, 399 Royal Parade, Parkville, VIC 3052, Australia. E-mail: celine.valant@monash.edu